Article:

Kudzotsa, I, Phillips, VTJ and Dobbie, S (2016) Aerosol Indirect Effects on Glaciated Clouds. Part II: Sensitivity Tests Using Solute Aerosols. Quarterly Journal of the Royal Meteorological Society, 142 (698 A). pp. 1970-1981. ISSN 0035-9009

https://doi.org/10.1002/qj.2790

Aerosol Indirect Effects on Glaciated Clouds. Part II: Sensitivity Tests Using Solute Aerosols†

Innocent Kudzotsa*,[a] Vaughan. T. J. Phillips, [b] Steven Dobbie, [c]

[a]*Department of Physics, University of Zimbabwe, MP 167 Mt Pleasant, Harare, Zimbabwe*

[b]*Department of Physical Geography and Ecosystem Science, Sölvegatan 12, S-223 62, Lund, Sweden*

[c]*School of Earth and Environment, University of Leeds, Leeds, UK*

*Correspondence to: *ikudzotsa@science.uz.ac.zw*: Department of Physics, University of Zimbabwe, MP 167 Mt Pleasant, Harare, Zimbabwe

Sensitivity tests were performed on a mid-latitude continental case using a state-of-the-art aerosol-cloud model to determine the salient mechanisms of aerosol indirect effects (AIE) from solute aerosols. The simulations showed that increased solute aerosols doubled cloud droplet number concentrations, and hence reduced cloud particle sizes by about 20 % and consequently inhibited warm rain processes, thus, enhancing chances of homogeneous freezing of cloud droplets and aerosols. Cloud fractions and their optical thicknesses increased quite substantially with increasing solute aerosols. Although liquid mixing ratios were boosted, there was however a substantial reduction of ice mixing ratios in the upper troposphere owing to the increase in snow production aloft. The predicted total aerosol indirect effect was equal to -9.46 $\pm$ 1.4 Wm^{-2}. The AIEs of glaciated clouds (-6.33 $\pm$ 0.95 Wm^{-2}) were greater than those of water-only clouds (-3.13 $\pm$ 0.47 Wm^{-2}) by a factor of two in this continental case. The higher radiative importance of glaciated clouds compared to water-only clouds emerged from their larger collective spatial extent and their existence above water-only clouds. In addition to the traditional AIEs (glaciation, riming and thermodynamic), sedimentation, aggregation and coalescence were new AIEs identified.

Key Words: Aerosol-cloud interactions; Cloud microphysics; Cloud-resolving models; Glaciated clouds; Indirect effects; Clouds; CLASIC.

Received . . .

1. Introduction

The industrial revolution and subsequent growth in manufacturing output worldwide, has led to an increased background aerosol concentration relative to pre-industrial times (Watson et al. 1990; Andreae et al. 2007; Takemura 2012). Although, the upward trend of the global average of aerosol pollution continues primarily due to growing economies in Asia, particularly China and India (Streets et al. 2003; Ramanathan et al. 2007), most of the developed countries have already reached their peak in emitting anthropogenic aerosols (Takemura 2012). Pollution due to biomass burning also continues to rise, particularly in the southern hemisphere (Andreae and Merlet 2001; Takemura 2012). These anthropogenic changes in atmospheric aerosol loading especially of sulphate and carbonaceous aerosols, have substantially altered the chemistry and loading of the natural aerosol field (Sun et al. 2004; Salma and Maenhaut 2006).

According to the Intergovernmental Panel on Climate Change (IPCC) reports (Solomon et al. 2007; Boucher and Randall 2013), aerosols are one of the major climate forcing agents; they do so via two major pathways. Firstly, by the *aerosol direct effect* whereby aerosols scatter and absorb shortwave radiation and also absorb and re-emit longwave radiation in different directions, thereby altering the radiation budget of the Earth (Charlson et al. 1992; Liao and Seinfeld 1998). The other pathway, which is the subject of this work is when aerosols act first, as Cloud Condensation Nuclei (CCN) or Ice Nuclei (IN). This implies that their changes in chemical composition and number or mass concentration may lead to modifications in clouds' microphysical and optical properties, thus, altering the Earth's radiation budget (Albrecht 1989). This second mechanism is referred to as the *aerosol indirect effect (AIE)* (Charlson et al. 1992; Haywood and Boucher 2000; Lohmann and Feichter 2005; O'Donnell et al. 2011; Gettelman et al. 2012). There is also the *semi-direct* effect, which is caused by absorbing aerosols (Lohmann and Feichter 2001; Johnson et al. 2004). These absorbing aerosols have a heating effect in the atmosphere, which may subsequently cause the evaporation of cloud particles (Johnson 2003; Hill and Dobbie 2008; Koch and Genio 2010).

†

It is important to study the many and varied indirect influences of aerosols on clouds, because clouds control the radiation budget of the Earth (Hobbs 1993; Liou 2002; Lohmann and Feichter 2005; Solomon et al. 2007), yet how they will respond in future to changes in aerosol chemistry and loading, remains conjectural, and this potentially emerges as the greatest source of uncertainty in climate prediction (Bony and Dufresne 2005; Baker and Peter 2008; Phillips et al. 2008; Fan et al. 2012; Boucher and Randall 2013). Initial work in this area shows that AIE are potentially very important, particularly in offsetting the carbon dioxide (CO_2) induced global warming (Twomey 1974, 1977; Albrecht 1989; Leaitch et al. 1992).

Although, several observational, modeling and laboratory studies on aerosol-cloud interactions have been carried out in the past, most of them have focused on warm clouds (Martin et al. 1994; Cui et al. 2006; Hoeve et al. 2011; Costantino and Br9on 2013). Consequently, little is known about aerosol indirect effects of glaciated clouds (Gettelman et al. 2012). This is because there are large uncertainties in the measurements and knowledge of ice nucleating aerosols (Cziczo et al. 2004; DeMott et al. 2011) and also in the mechanisms of ice nucleation at different temperatures and humidity (Meyers et al. 1992; Phillips et al. 2008; Eidhammer et al. 2009). Hence, this study proposes to contribute to the knowledge of aerosol-cloud interactions (aerosol indirect effects) on glaciated clouds by way of sensitivity tests, using a state-of-the-art aerosol-cloud model (Phillips et al. 2007, 2008, 2009; Kudzotsa 2013; Kudzotsa et al. 2016) that encapsulates a tested and robust heterogeneous ice nucleation scheme of Phillips et al. (2008, 2013), which treats all the four known modes of heterogeneous ice nucleation (Diehl et al. 2001, 2002; Hoppel et al. 2002; Dymarska et al. 2006). The details of this model have been described in full in part I of this series of papers (Kudzotsa et al. 2016).

The focus of this study was on investigating the diverse mechanisms for aerosol indirect effects via glaciated clouds from anthropogenic emissions of soluble aerosols. Here we outline the overarching aims and objectives set out for this study and describe their respective hypotheses that were being tested. We explore on the meso-scale, the cloud microphysical and dynamical mechanisms for glaciated-cloud indirect effects from anthropogenic soluble aerosols. In this study, the term glaciated-cloud refers to clouds with any form of ice in them, either as mixed phase or completely glaciated clouds. The hypothesis being tested here is that, solute aerosols modify glaciated clouds via the homogeneous freezing process of cloud droplets and of solute aerosols. Also, reduced sedimentation rates produce a lifetime effect, causing pollution by solute aerosols to modify cirrus clouds more than solid aerosols, owing to the much higher numbers of soluble aerosols relative to insoluble ones. We also explore the *riming effect*, which is caused by the reduction of droplet sizes due to an increase in the droplet number concentration and the freezing-related *thermodynamic or invigoration* aerosol indirect effect due to latent heat release during the freezing of extra cloud droplets. The hypothesis being tested here is that, the thermodynamic and the riming indirect effects from soluble aerosols are significant, but do not dominate the total indirect effect on all clouds (warm and cold).

The structure of this article is as follows. In Section 2, the experiments conducted in this study to assess and quantify the different types of aerosol indirect effects are described. The results from the two cases simulated are given and analyzed in Section 3. Finally, conclusions and future work will be stated in the last section, which is Section 5.

2. The Set-up of the Experiments

The approach for verifying or disproving these scientific hypotheses in this meso-scale modeling study was to perform sensitivity tests using the simulations of a case of deep convection from the atmospheric and radiation measurement (ARM) site, the mid-latitude continental case, the Cloud and LAnd-Surface Interaction Campaign (CLASIC), which was carried out over the Southern Great Planes (SGP) in Okhlahoma, U.S.A. during the northern hemisphere summer of 2007 (Miller 2007) (lat = 36.61° and lon = 97.49°). CLASIC was a three-weeks long continental campaign studying deep convection, which was carried out from the 10th to the 30th of June in 2007, which is the same duration for which the simulations were conducted. The details of this campaign are given in part I of this work (Kudzotsa et al. 2016). The experiments were conducted as follows.

Soluble Aerosol material	Adjustment Factor
Ammonium Sulphate (SO4)	0.19
Sea-Salt (SS)	1.
Soluble Organics (SO)	0.67

Table 1. *Fractional changes of soluble aerosol scenarios from pre-industrial (1850) to present-day (2000) number and mass distributions (inferred from Takemura (2012)).*

The control run for the simulated case was specified as described in Kudzotsa et al. (2016), and was simulated using present-day aerosol scenarios and thermodynamic conditions for model forcing. In order to specify the pre-industrial aerosol fields, the work of Takemura (2012) on the global distribution of atmospheric aerosols from the pre-industrial era (1850) to future projections (2100) (using global models) was used. An adjustment factor for each particular aerosol group in the model (Table 1) was inferred from Takemura (2012). Sulphate is the most affected aerosol specie and increased by a factor of five from pre-industrial times. All organics (soluble and insoluble species) have gone up by approximately 50%, while the number and mass concentrations of soot were boosted by a factor of over three. Dust and sea-salt have the least changes among all the aerosol species. These adjustment factors were used to estimate the corresponding pre-industrial aerosol number and mass distributions.

There is however uncertainties with our assumptions of the adjustment factors when estimating our preindustrial aerosol scenarios, mainly because these are derived from model simulations, which may not be perfect. Other researchers (e.g. Morrison and Grabowski (2011); Fan et al. (2013)) have applied a single arbitrary factor (e.g. 6 in the case of Fan et al. (2013)) to all aerosol species when estimating their pre-industrial aerosol concentrations and this shows that there is no unique way of prescribing the pre-industrial aerosol concentrations.

The changes in aerosol concentrations and chemistry between the pre-industrial and the present-day simulations in this study will induce an aerosol indirect effect only as the direct effect was not activated in the GFDL radiation scheme used.

2.1. Test A: The Total and Albedo-Emissivity Aerosol Indirect Effects

2.1.1. The total aerosol indirect effects

The principal objective here is to assess the role that anthropogenic solute aerosols have played in modifying the properties of all clouds from pre-industrial times to present-day, by their initiation of cloud droplets via either condensation or homogeneous freezing. This is done by conducting a pair of model simulations – one for the present-day aerosol scenario (PDCTRL, which is the control simulation), while the other one is with a pre-industrial solute aerosol burden (PINSOL, i.e., without anthropogenic solute aerosols). These simulations are performed using present-day thermodynamic conditions for the model forcing. This was designed to eliminate any radiative forcings that would arise from changing the thermodynamic forcing, hence, this flux change cannot be compared directly with traditional radiative forcings that are not aerosol induced. The difference in the net radiative fluxes at TOA (evaluated at the model top, which is roughly at 20 km altitude) between the control simulation, F_{PDCTRL}, and pre-industrial simulation, F_{PINSOL} becomes the total *aerosol indirect effect* or simply the *net change in the radiative fluxes at the TOA*, F_{net}, in Eqn 1. This is a standard technique that has been applied by other researchers in previous studies (e.g. Gettelman et al. (2012); Lohmann et al. (2010); Haywood et al. (2009)) albeit in global studies of aerosol indirect effects using GCM.

$$F_{net} = F_{PDCTRL} - F_{PINSOL} \tag{1}$$

2.1.2. The albedo-emissivity aerosol indirect effects of glaciated clouds

The radiation scheme used herein is the GFDL radiation scheme (Freidenreich and Ramaswamy 1999), and does not treat the direct effect of aerosols. Cloud particle mean diameters and net radiative fluxes are respectively the inputs and outputs to this scheme. These mean sizes are required by the radiation scheme as inputs to calculate the shortwave and longwave scattering properties of clouds. Therefore, in order to determine the albedo-emissivity aerosol indirect effect of a targeted cloud type, two model runs are performed (PDCTRL and PINSOL), each with two calls to the radiation scheme.

The first calls are the normal calls necessary for treating the interaction between atmospheric radiation and the meteorology of the simulation. The difference in the net radiative fluxes at TOA between the control and the pre-industrial simulations determined using the these first calls to the radiation scheme gives the total of effective net radiative flux, $F_{net} = F_{eff}$ as described above.

On the other hand, the second call to the radiation scheme is made for diagnostic purposes only (i.e., it does not alter the microphysics of the model). In the second call, the sensitivity of clouds to changes in aerosols is eliminated by using temperature-dependent look-up tables of the mean sizes of cloud droplets and ice crystals instead of the predicted mean sizes. These look-up tables are created from the control run (PDCTRL described above), but they could equally be created also from the pr-industrial run. The same look-up tables are used for both PDCTRL and PINSOL runs. The difference in the net radiative fluxes at TOA between the control and the pre-industrial simulations determined using the these second calls to the radiation scheme gives a hypothetical net radiative flux, F_{hyp}. Finally, subtracting F_{hyp} from F_{eff}, gives us the estimate of the total albedo-emissivity effect from clouds, F_{alb}.

In order to determine the total lifetime indirect effect from clouds, F_{lif}, the albedo-emissivity effect, F_{alb} is subtracted from F_{eff}. If this technique is applied to a targeted cloud type or group by using their corresponding look-up tables, then their cloud albedo-emissivity and cloud lifetime effects can be estimated.

2.1.3. Albedo-emissivity of Ice-only and Mixed-Phase Clouds

A model grid point was defined as containing ice-only clouds when at any given time-step, the mixing ratio of cloud droplets was not greater than zero when that of cloud ice was greater than zero. Mixed-phase clouds on the other hand were defined when the mixing ratios of both cloud droplets and cloud ice were greater than zero at the same time-step and grid-point. The same criterion was used for the definition of water-only clouds.

The albedo-emissivity effect of ice-only clouds is inferred by fixing the mean sizes of ice crystal via the use of look-up tables in completely glaciated clouds only. This is performed by using the second call to the radiation scheme as described above. For mixed-phase clouds, the mean sizes of ice crystals are fixed only in mixed-phase clouds during the second call to the radiation scheme. This analysis of the output was designed to investigate the proportional contributions of the ice and liquid components of mixed-phase clouds to the albedo emissivity effect of mixed-phase clouds.

2.2. *Test B: Isolating Lifetime Indirect Effects for Glaciated Clouds*

In this test, indirect effects from aerosols on liquid-only clouds are eliminated first. This is done by using look-up tables of droplet numbers or, of droplet mean sizes to eliminate the sensitivity of certain microphysical processes to changes in aerosol loading. These microphysical processes are the *auto-conversion, collision-coalescence, sedimentation* and the optical properties of clouds, because in nature, all these processes depend on the mean size of cloud particles. Therefore, by simultaneously fixing the number concentrations or mean sizes of cloud-droplets in all these processes, the response of the lifetime of water clouds to solute aerosol pollution could be eliminated from the meteorology of the simulation.

These look-up tables are temperature and vertical velocity dependent, since our cloud droplet nucleation scheme is a function of temperature and vertical velocity and are created from the control simulation. The same look-up tables are used for both the present-day (PDCTRL) and the pre-industrial (PINSOL) runs.

The difference in the net radiative fluxes at TOA between the control and the pre-industrial simulations determined using look-up tables to these microphysical processes gives a hypothetical net radiative flux without the lifetime effects of water-only clouds, $F_{hyp-lif-wat}$. Finally, subtracting this $F_{hyp-lif-wat}$ from F_{eff} determined in Test A, gives us the estimate of the lifetime effect from glaciated clouds.

2.2.1. *Test B.1: Aerosol Indirect Effects of Ice-only Clouds*

In order to isolate aerosol indirect effects on ice-only clouds from the total indirect effects of glaciated clouds, the responses of the aerosol dependent microphysical processes of ice-only clouds are eliminated from the simulation to only allow responses from aerosol dependent processes of mixed-phase and liquid-only clouds to control the aerosol indirect effects of the simulation. In this test, the mean sizes of ice crystals in ice-only clouds are fixed again in both PDCTRL and PINSOL simulations by using look up tables similar to those used above, but now only in aerosol dependent microphysical processes of ice-only clouds, such as auto-conversion of cloud ice to snow, aggregation of snow and cloud ice, aggregation of graupel and cloud ice, sedimentation of cloud ice and their radiative processes.

This eliminates the contribution of ice-only clouds to the total indirect effect of aerosols from all clouds, hence, the difference in the net radiative fluxes at TOA between the control and the pre-industrial simulations determined using look-up tables gives a hypothetical total aerosol indirect effect without the ice-only clouds aerosol indirect effect, $F_{hyp-lif-wat-mix}$. If this, $F_{hyp-lif-wat-mix}$ is subtracted from the total aerosol indirect effect, F_{net}, estimated in Test A, then the ice-only clouds aerosol indirect effect is determined.

2.2.2. *Test B.2: Aerosol Indirect Effects of Ice in Mixed-phase Clouds*

Since we now have the aerosol indirect effects of glaciated clouds from Test B and the ice-only clouds indirect effect from Test B.1, then the mixed-phase clouds aerosol indirect effect can be determined by subtracting the aerosol indirect effect of ice-only clouds from that of glaciated clouds clouds.

2.3. *Test C: Investigating the Riming Indirect Effect*

Here, we test the hypothesis that soluble anthropogenic aerosols induce a riming effect by reducing the mean sizes of cloud droplets and reducing the efficiency with which supercooled cloud droplets are collected by solid hydrometeors. In order to evaluate this phenomenon, the same look-up tables of the cloud droplet sizes with dependencies on temperature and vertical velocity are utilized to fix droplet sizes in the riming routines of the microphysics scheme, for both the PDCTRL and the PINSOL simulations.

What we get here after applying Eqn. 1 for these simulations is a hypothetical TOA glaciated clouds flux change without the riming effect, $F_{hyp-gla-rim}$. By subtracting this hypothetical, $F_{hyp-gla-rim}$ from the actual glaciated clouds flux change in Test B, we get the riming indirect effect.

2.4. *Test D: Investigating the Freezing-Related Thermodynamic Indirect Effect*

The hypothesis being tested here is that, the thermodynamic, riming and glaciation indirect effects from soluble and solid aerosol are significant but do not dominate the total AIE on all clouds. This is executed by repeating Test A, but with all temperature adjustments that arise from the latent heating released during all ice involving phase changes (e.g. freezing and melting) being switched off.

By using Eqn. 1 for the two simulations we get a hypothetical total aerosol indirect effect but without the thermodynamic indirect effect, $F_{hyp-net-ther}$. Hence, if we subtract this hypothetical indirect effect, $F_{hyp-net-ther}$ from the true total cloud indirect effect, F_{net} estimated from Test A, the thermodynamic aerosol indirect effect is determined.

3. Results From the Mid-latitude Continental Case (CLASIC)

3.1. *Response of Cloud Microphysical Properties to Increased Solute Aerosols*

Two model runs described in Test A were performed, here we analyze the results in order to understand the underlying mechanisms of aerosol indirect effects caused by changes of solute aerosol scenarios from pre-industrial to present-day. In most of the analysis plots presented in the following sections, two curves are used; the red curve represents the present-day aerosol conditions (PDCTRL), while the blue curve represents the pre-industrial aerosol conditions (PINSOL), unless it is specified in the text.

3.1.1. *Cloud Droplet Concentrations and their Mean Sizes*

Figure 1a compares the droplet number concentration between the pre-industrial and present-day simulations. These prognostic variables are conditionally averaged over all cloudy regions and the entire simulation period and in this analysis, a cloudy grid-box was defined as a grid-box with either cloud ice or cloud liquid. It is noticeable that the control run reported significantly more cloud droplets than the corresponding pre-industrial continental run by nearly a factor of two. This outcome shows the non-linearity of the CCN activity of aerosols when compared to the net aerosol perturbation that was applied, e.g. sulphate aerosols were increased by approximately a factor of five from pre-industrial to present-day.

One explanation for this doubling of the droplet number concentration is the inability of other anthropogenic solute aerosols to act as CCN under the prevailing meteorological conditions, because the shape of the aerosol size distribution are kept the same in both simulations. As a result, competition effects are exacerbated when CCN concentrations are increased and more CCN tend to lower the critical supersaturation for CCN activation. Also, cloud droplets initiated at the cloud-base were higher in the present-day, hence, supersaturations are decreased more quickly. Thus, in-cloud nucleation of cloud droplets may subsequently be less prolific.

It is the thermodynamical state of the atmosphere (which was maintained the same in these two simulations) that determines the water content of a cloud, not the aerosol loading. Therefore, aerosol pollution triggered competition for available water vapor by extra cloud particles, leading to their smaller mean sizes. This reduction in cloud droplet mean sizes is reviewed in Fig. 1b, which shows that droplets have become smaller (by about 4 microns $\approx$ 20%) due to anthropogenic pollution. These current results corroborate the findings of several previous observational and modeling workers, for instance, Twomey (1974); Albrecht (1989); Phillips et al. (2003) noted reductions of mean sizes of cloud droplets with increasing aerosol number concentrations, such as the anthropogenic increase of aerosol from preindustrial times to present-day in our case. More recently, Pandithurai et al. (2009) noted similar trends when they performed a series of local scale

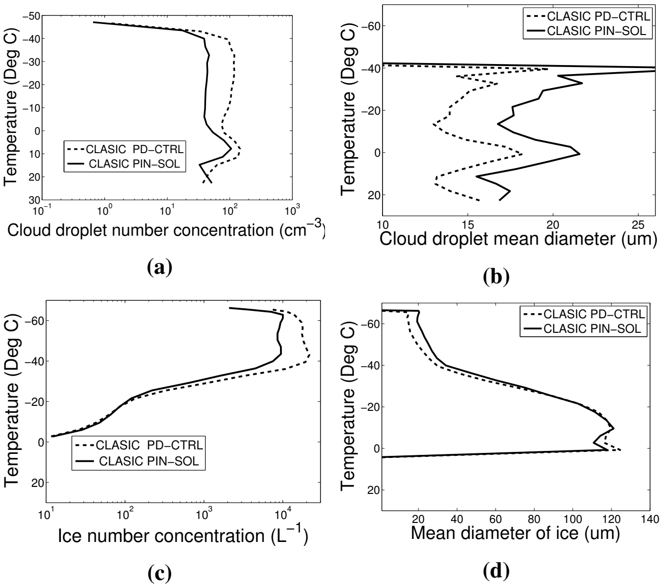

Figure 1. *(a) Cloud droplet number concentrations (cm^{-3}), (b) cloud droplet mean diameter in μm, (c) ice Crystal number concentration (L^{-1}) and (d) ice crystal effective radius (μm), all conditionally averaged over cloudy region (right)*

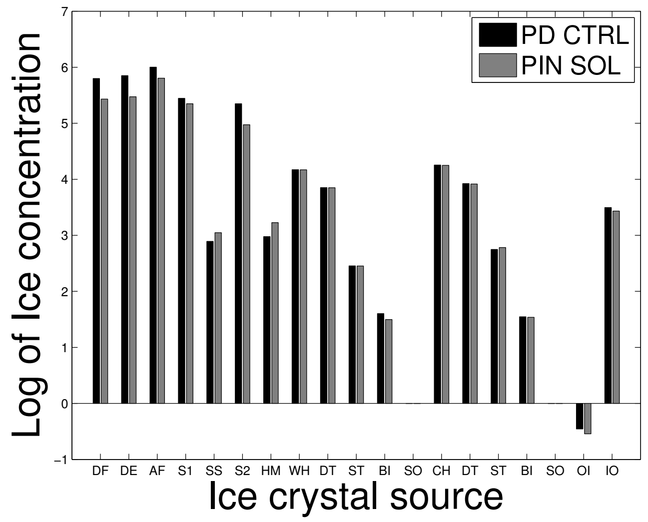

Figure 2. *The budget of ice number from the effect of solute aerosols for the mid-latitude continental case (CLASIC). Meanings of abbreviations in (d) DF = droplets frozen homogeneously, DE = droplets evaporating during homogeneous freezing, AF = aerosols frozen homogeneous, (S1, SS, S2) droplets in 1st mode of SO4, sea-salt, 2nd mode of SO4 aerosols, respectively, that froze homogeneously. HM = H-M splinters, WH = total crystals from Warm Heterogeneous nucleation (Condensational, Depositional, and Immersion at temperatures > -30 °), (DT, ST, BO, SO) crystals by Warm Heterogeneous nucleation of dust, soot, biological organics and soluble organics, respectively. CH = total crystals from Cold Heterogeneous nucleation (Condensational, Depositional, and Immersion at temperatures < -30 °), (DT, ST, BO, SO) crystals by dry deposition from dust, soot, and biological organics and soluble Organics, respectively. Finally, OI and IO stand for total ice crystals from Outside-In and Inside-Out Contact freezing.*

observational campaigns, using surface-based remote sensing systems during episodic events of increased CCN concentrations.

3.1.2. Ice Crystal Concentrations and their Effective radii

The core hypothesis of this part of the investigation is that anthropogenic solute aerosols modify ice clouds through homogeneous freezing. This postulation is explainable through Fig. 1c in which the ice crystal number concentrations per liter are presented. There is a substantial increase of upper tropospheric ice crystal concentrations above -40°C (the 9 km altitude) of almost a factor of 2. This increase is evident despite that in the aerosol-cloud model used in this study, solute aerosols are not treated as primary sources of ice crystals in terms of heterogeneous nucleation. This leaves homogeneous freezing responsible for the increase of ice crystal concentrations aloft.

Apparently, no cloud droplets also exist beyond the -40°C temperature level (Fig. 1a), which is the homogeneous freezing level. This shows that the extra cloud droplets in the present-day run contributed to the simulated extra ice crystals aloft when they froze homogeneously. However, the fractional increase in ice crystal concentrations is mild when compared to the fractional increase in droplet number concentration (Figs. 1a and 1c). This discrepancy in their fractional increases is due to the increase in the number of droplets that evaporated during homogeneous freezing as noted from the ice crystal number budget (Fig. 2, bars DE).

Figure 2 shows the ice number budget of the various sources of ice crystals treated in the model. The bar chart shows that the droplet and aerosol freezing are the major sources of cloud ice. And in terms of aerosols freezing, sulphate aerosols dominate the sources because of their large number concentrations relative to other aerosols in the atmosphere. As for heterogeneous ice nucleation, dust dominates the sources followed by soot, while biological aerosols nucleate very little ice. The treatment of homogeneous freezing in the microphysics scheme follows the treatment of the process by Phillips et al. (2007) in which, homogeneous freezing of large cloud droplets ensues first, allowing for evaporation of smaller cloud droplets and vapour growth of new crystals depending on ice supersaturation.

A slight reduction of the effective sizes of ice crystals (of about 5 microns ≈ 15%) is noticeable in the upper troposphere commencing from the level of homogeneous freezing (Fig. 1d). The dominant mechanism for this reduction is the competition for available water vapour by extra ice crystals from homogeneous freezing. The second mechanism is the low deposition coefficient (which is a measure of how efficiently excess vapor is taken up by

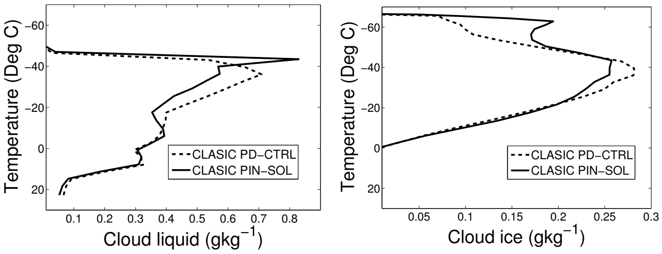

(a) (b)

Figure 3. *Cloud mass-mixing ratios, (a) liquid-cloud mass mixing ratio unconditionally averaged in all clouds and (b) ice-cloud mass mixing ratio unconditionally averaged in all clouds for the CLASIC case.*

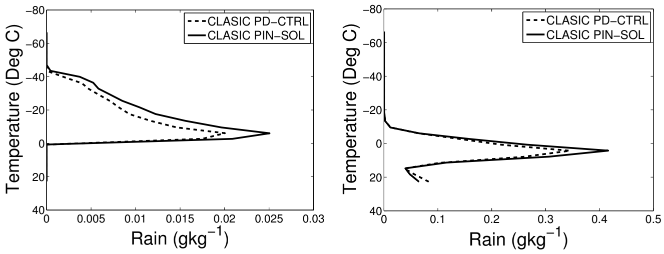

(a) (b)

Figure 4. *(a) Rain mass-mixing ratios in mixed-phase and (b) in liquid-only clouds, unconditionally averaged over the whole domain and simulation period for the CLASIC case.*

growing ice particles) that characterizes some of the ice crystals, hence, the amount of vapour transfer to the ice phase is reduced (Gao et al. 2004). Also, faster sedimentation of larger ice crystals due to the influence of gravity on larger particles compared to smaller particles can explain why small sizes are predicted aloft.

The other finding emerging here is the increase of mean sizes of ice crystals in the lower troposphere (typically, mixed-phase clouds). This finding is interesting because it contradicts with the generally accepted concept that pollution of a cloud by aerosols should reduce the sizes of cloud droplets. The predicted increase in the mean sizes of ice crystals can be explained by the Bergeron-Findeisen process of ice crystals sedimenting from the anvil outflow down to the mixed phase regions of the clouds where supersaturations may be higher.

3.1.3. Water Contents

.

The data from Figs. 3a and 3b highlight the mass mixing ratios of clouds. The liquid and ice mixing ratios are less sensitive to changes in aerosol loading especially in the lower troposphere. In the mixed-phase region of clouds, both liquid and ice water mass are however, significantly higher in the present-day than in the pre-industrial era, while the ice mixing ratios of cirrus clouds is lower in the present-day. The increase in both liquid and ice water contents is dominantly linked to the increase in mixed-phase cloudiness and a reduction in rain production (Fig. 4a), while, the reduction in ice water content is attributed to the surge in the unconditionally averaged snow mass mixing ratio aloft (Fig. 5c). Another discovery from the two figures is the tendency of increasing sensitivity to changes in aerosol loading with increasing height. This is explicable in terms of in-cloud activation of droplets by small aerosols in deep convective updrafts, which accelerate aloft. Continental air has many such small aerosols that can activate aloft (warm rain process would tend to cause a reduction of sensitivity with height).

3.1.4. Precipitation from the Warm Rain and Ice-Crystal Processes

In the aerosol-cloud model used here, warm rain is produced mainly by auto-conversion and collision-coalescence processes. These processes largely control the rain mass mixing ratio in mixed-phase and water only clouds. Rain mass-mixing ratio is a powerful parameter to diagnose the precipitation producing efficiency of a cloud. A significant reduction in rain mixing ratio in the present-day simulations is apparent especially in mixed-phase clouds, because of the increase in the glaciation of clouds with increasing aerosol concentrations (Figs. 4a and 4b).

Although the dominant mechanism for the suppressed rain production in the present-day is the collision-coalescence process which is less effective due to smaller sizes of cloud droplets (Fig. 1b). There are; however, other secondary mechanisms for this reduction in rain mixing ratios. The first secondary mechanism is the repartitioning of condensate from rain to snow, because in the present-day, more ice crystal are being produced owing to homogeneous freezing of cloud droplets and aerosols. Hence, more snow is being produced leading to the depletion of the liquid phase by the ice-phase (Fig. 5). This phenomenon due to changes in atmospheric conditions that tend to favour the formation of snow over rain as explained by Lohmann and Feichter (2005) and also noted by Zeng et al. (2009). Another mechanism for this finding is the proliferation of ice crystals aloft - ice crystals, snow pellets or graupel particles subside from anvil outflow, into mixed-phase clouds, and exhaust the liquid mass, via the 'Bergeron-Findeisen' process.

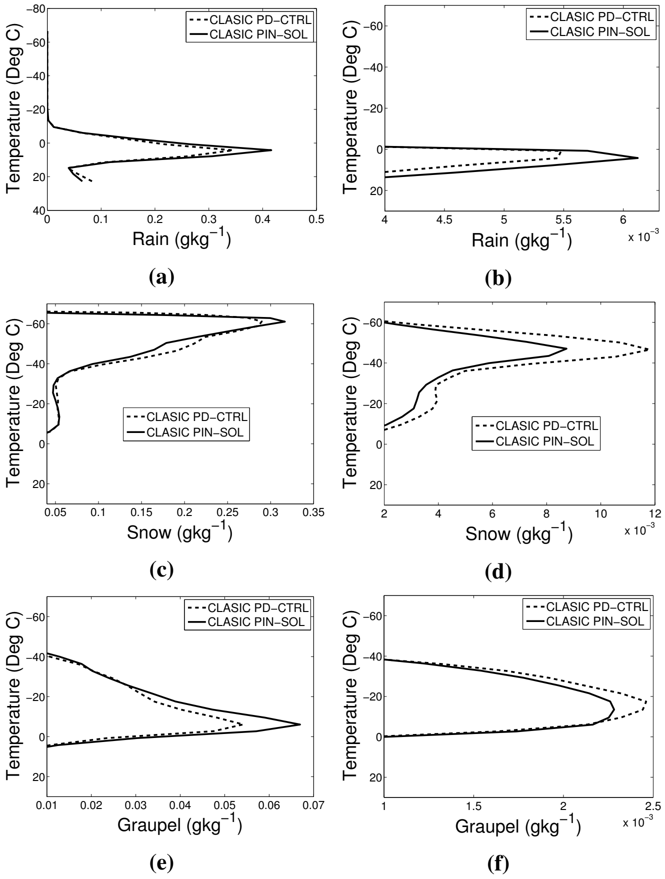

Figure 5. *(a and b) Rain mass-mixing ratios, (c and d) Snow mass-mixing ratios and (e and f) Graupel mass-mixing ratios. Figures on the left represent profiles of conditional averages over cloudy regions, while those on the right represent profiles of unconditional averages over the whole domain and simulation period for the CLASIC case.*

Precipitation production in the ice phase has increased in the present-day via snow production aloft, although the intrinsic mass mixing ratio of snow in all clouds was somehow insensitive to increased aerosols (Fig. 5c), unconditional average of snow mixing ratio over the whole simulation shows a significant increase in snow production when solute aerosol concentrations were raised (Fig. 5d). These contrasting responses suggest that, intrinsically, the average snow production by clouds was unchanged, although the snow-producing clouds became more extensive. This discovery is supported by the cloud fraction statistics shown (Sect. 3.3). This increase in domain-wide snow production is responsible for the reduction in ice mixing ratio aloft. The average graupel production by clouds diminished in the present-day (Fig. 5e), primarily because of small cloud droplets, however, the increase in cloud extent with increasing aerosol burden caused an increase in domain-wide graupel production (Fig. 5f).

3.2. Response of Cloud Dynamical Properties to Increased Solute Aerosols

Unexpectedly, updrafts with vertical velocities greater than 1m s^{-1} were weakened by aerosol pollution in the free troposphere (Fig. 6a). This outcome was attributed to increased gravitational burden caused by increased condensate loading particularly in mixed-phase clouds (Figs. 3). Previous researchers e.g. Storer and van den Heever (2013) and Cui et al. (2006) also detected similar trends, especially in deep-convective clouds. As for weak vertical velocities, a strengthening of vertical velocities was evident especially in the upper troposphere (Fig. 6c), and this strengthening was attributed to latent heat release during homogeneous freezing of extra cloud droplets. Downdrafts have shown weak sensitivities to increased aerosols, although a significant strengthening of weak downdrafts was predicted (Figs. 6b and 6d). Surging gravitational burden as well as evaporative cooling from falling hydrometeors can cause strengthening of downdrafts.

Evidence of the thermodynamic effect (Test D) is quite significant in Fig. 7a, which demonstrates the change in predicted mean atmospheric temperature from pre-industrial to present-day aerosol scenario. It is apparent that, the mean atmospheric temperature increased by as much as 0.5°C in the upper troposphere. This finding is principally attributed to the release of latent heat during homogeneous freezing. The fact that the temperature change is maximum at the homogeneous freezing level is consistent with the fact that homogeneous freezing of aerosols and cloud droplets is the cause. The cooling near the 0°C level is attributed to evaporative cooling caused by precipitating hydrometeors as supported by the increase in relative humidity at about the same altitude (Fig. 7b). The predicted reduction of relative humidity in the upper troposphere (Fig. 7b) arises mainly from increased competition for vapour by extra ice crystals, increased snow production and subsequent decrease of ice-only cloud mass.

3.3. *Response of Cloud Extent to Increased Solute Aerosols*

3.3.1. *Horizontal Cloud Fraction*

Looking at the broader properties of the clouds across the simulation domain, described as the macrophysical features, Fig. 8 shows changes in domain-averaged cloud fractions. This is the fraction of the horizontal area of the domain covered by grid-columns that have cloud in them. On the other hand, Fig. 9 shows the change in volumetric cloud fraction. The volumetric cloud fraction is the fraction of the volume of the whole domain and entire simulation period that is occupied by clouds. Therefore, Fig. 8 illustrates the degree of changes in the horizontal extent of clouds, whereas Fig. 9 encapsulates the lifetime component and mass budget of the clouds by including changes in vertical, as well as horizontal, extent.

A distinct increase in the fractions of all cloud regimes was simulated by the present-day run relative to the pre-industrial simulation. The largest changes in horizontal coverage are in mixed-phase clouds followed by ice-only clouds (Fig. 8), while the volumetric cloud fraction also shows increases in the extent of mixed-phase and ice-only clouds, the largest increase is in ice-only clouds followed by mixed-phase clouds (Fig. 9). This implies that ice-only clouds are now deeper than mixed-phase clouds. This indicates that some of the mixed-phase clouds in the present-day have been repartitioned to ice-only clouds. This happens because vapour growth of more numerous ice crystal from extra homogeneous freezing act to boost water subsaturation and evaporation of cloud-liquid (e.g. Korolev (2007)), especially in widespread regions of weak vertical velocities (stratiform clouds).

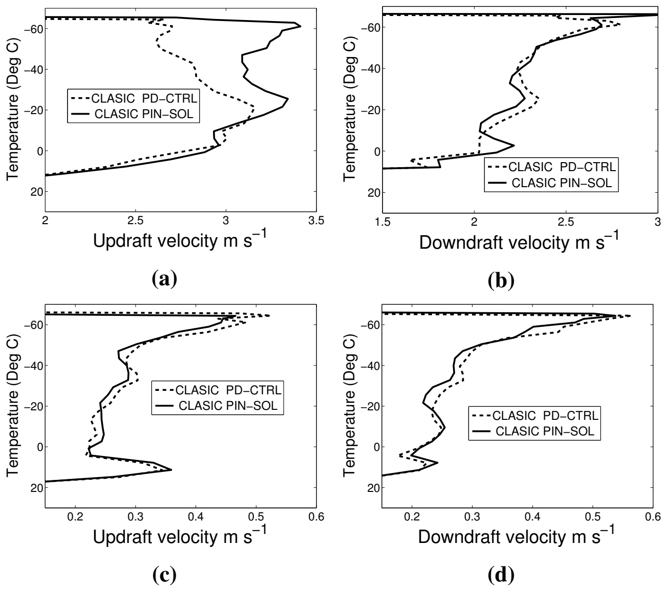

Figure 6. *Vertical profiles of positive (updrafts) and negative (downdrafts) ascent conditionally averaged over deep-convective clouds ($\omega > 1ms^{-1}$) and clouds with weak vertical velocities ($\omega < 1ms^{-1}$): (a) updrafts in strong vertical velocities, (b) downdrafts in strong vertical velocities, (c) updrafts in weak vertical velocities, (d) downdrafts in weak vertical velocities.*

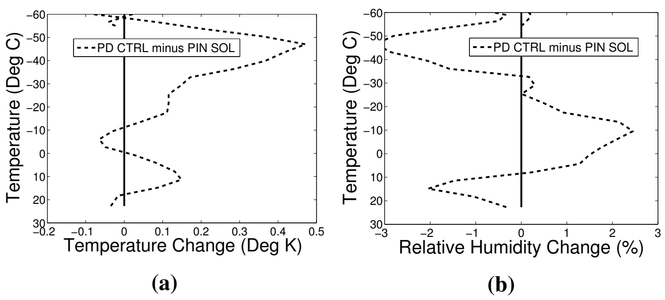

Figure 7. *PDCTRL-PINSOL unconditionally averaged mean change in (a) temperature and (b) relative humidity.*

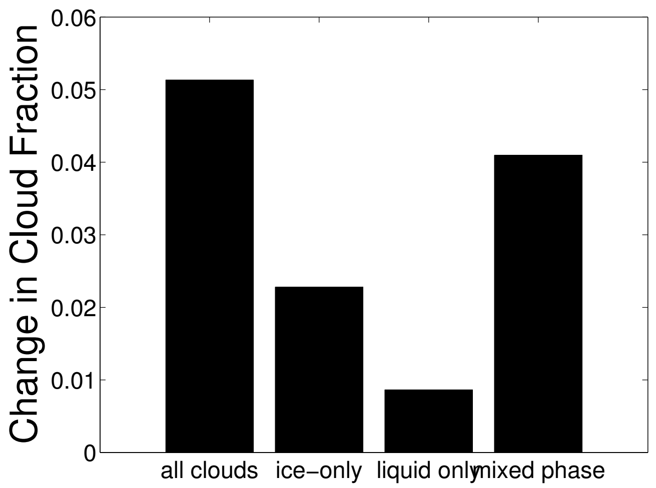

Figure 8. *Change in cloud fraction for all types of cloud species in the present-day simulation relative to 1800. A grid-column is defined as cloudy when the mass mixing ratio of either ice or liquid is greater than zero.*

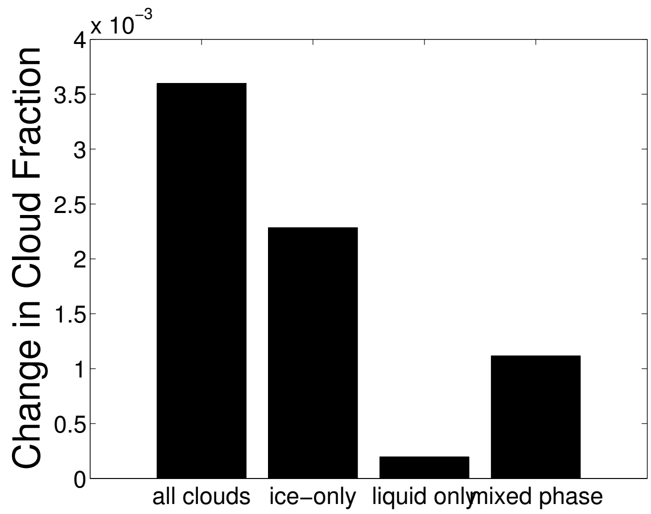

Figure 9. *Change in volumetric cloud fraction for all types of cloud species in the present-day simulation relative to 1800. A grid-column is defined as cloudy when the mass mixing ratio of either ice or liquid is greater than zero.*

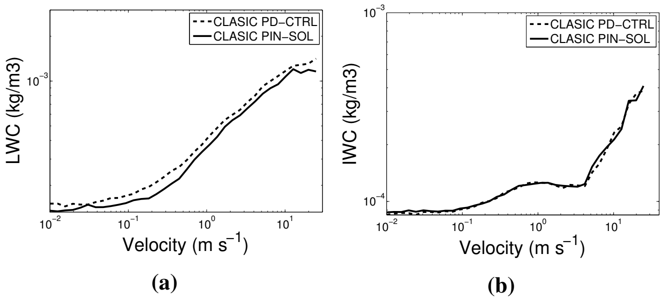

Figure 10. *Cloud properties as a function of vertical velocity conditionally averaged over cloudy regions, (a) Liquid Water Content, (b) Ice Water Content.*

3.4. Other Cloud Property Responses to Increased Solute Aerosols

Examining some of the cloud properties as a function of vertical velocity in each grid-box, Figs. 10a and 10b, show responses of cloud mass for a given velocity grid to changes in aerosol loading. On one hand, LWC is increased by aerosol pollution at all velocities, while on the other hand; IWC per each vertical velocity grid shows no sensitivity to changes in aerosol loading. The increase in LWC is reminiscent of the suppression of coalescence, which allows more liquid mass aloft to persist as indicated by the increase in cloud droplet number concentration.

3.4.1. Supersaturations

Another interesting phenomenon drawn from these results is the weakening of supersaturations over a cloud droplets due to increases in aerosol loading (plot not shown). This finding was attributed to the proliferation of cloud droplets, which compete more for excess vapour, since supersaturation is simply the balance between production and loss of excess vapour. This is why higher supersaturations were detected in maritime clouds than in continental clouds (Lamb and Verlinde 2011). Another factor contributing to the reduction in present-day supersaturations is the weakening of present-day strong updrafts.

3.5. Response of Cloud Optical Properties to Increased Solute Aerosols

It was shown from the simulations that clouds became denser in the present-day, because of the suppression of precipitation causing an increase the optical thickness (τ) of all cloud types.

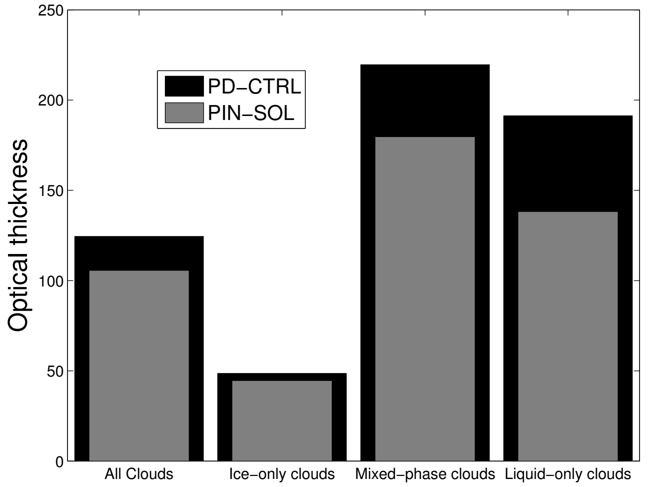

Figure 11. *Superimposed optical thicknesses predicted in the CLASIC simulation of mid-latitude continental clouds - conditionally averaged over grid-boxes in which the mass mixing ratio of a targeted cloud type is greater than zero. Optical depth from each cloud-type is plotted by assuming that no other cloud-types are present.*

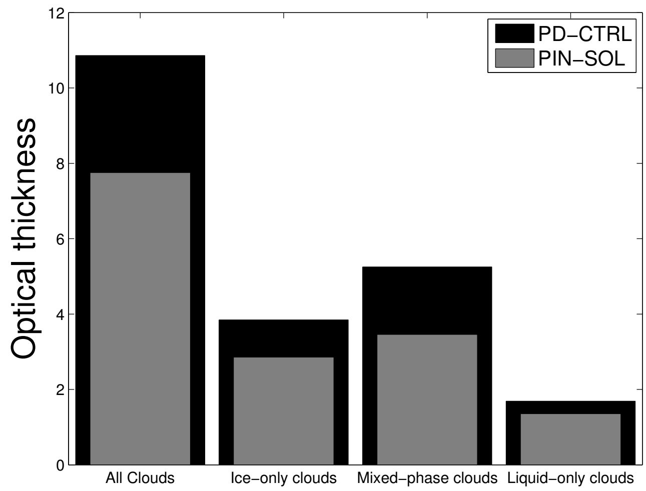

Figure 12. *Superimposed optical thicknesses predicted in the CLASIC simulation of mid-latitude continental clouds - unconditionally averaged of the entire domain and duration of the simulation. Optical depth from each cloud-type is plotted by assuming that no other cloud-types are present.*

The distinct increase in the domain averaged τ is also attributed to the predicted increase in the cloud fractions of all cloud types. Overall, all cloud phases were optically thicker in the present-day runs. The following conclusions were drawn about the optical thicknesses of the clouds. The responses of the intrinsic and the domain averaged optical thicknesses of clouds to changes in aerosols are presented in Fig. 11 and (Fig. 12, respectively.

- Liquid-only clouds are optically denser with increased aerosols but the response of domain-averaged optical thickness was minimal because, their horizontal cloud cover increased slightly.
- Mixed-phase clouds are more horizontally extensive and have higher water contents in the present-day, so their

optical thickness both conditionally and unconditionally averaged were greater.

- Ice-only clouds have similar optical properties per cloud, but are more horizontally extensive, so their net optical thickness throughout the domain increased.

4. Response of Radiative Fluxes and Cloud Radiative Properties to Increased Solute Aerosols

Figure 13 presents results of aerosol indirect effects via glaciated clouds from solute aerosols (PDCTRL - PINSOL), which were derived using the methods described in section 2. The full meanings of abbreviations used in the plot labels (of clusters of three bars) are given in the figure's caption. The total aerosol indirect effect is equal to -9.46 $\pm$1.4 Wm^{-2}. The total AIE, represented by the cyan bar in the bar chart, is the total change of net radiative fluxes at the TOA. The TOA radiative fluxes are unconditionally averaged over the whole domain and the indirect effects are estimated as described in test A.

The corresponding green bar represents the indirect effects of glaciated (mixed-phase plus ice-only) clouds (-6.33 $\pm$0.95 Wm^{-2}), while the red bar represents the aerosol indirect effects of water-only clouds (-3.13 $\pm$0.47 Wm^{-2}). The same glaciated cloud indirect effect bar appears again in the second cluster (glaciated cloud aerosol indirect effect (GC-AIE)) with its corresponding ice-only (magenta) (-4.14 $\pm$0.62 Wm^{-2}) and (blue) mixed-phase (-2.49 $\pm$0.37 Wm^{-2}) cloud components

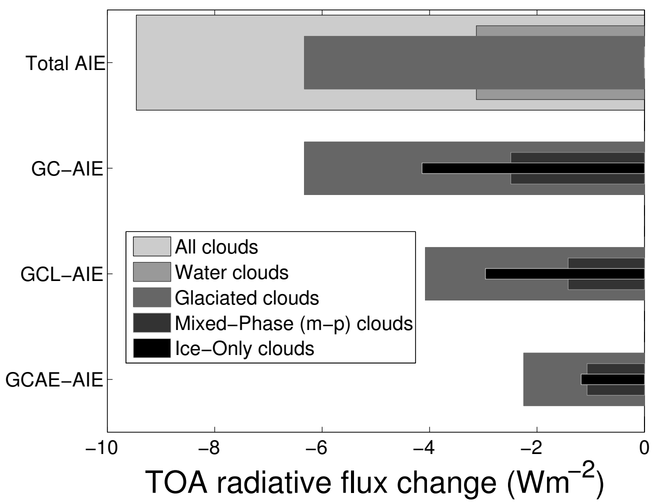

Figure 13. *Glaciated clouds aerosol indirect effects from solute aerosols (PDCTRL - PINSOL), results are derived mainly from tests A and B through identifying salient microphysical processes that are responsible for modifying cloud radiative properties in CLASIC. Meaning of abbreviations: GC-AIE = Glaciated Clouds AIE, GCL-AIE = Glaciated Clouds Lifetime AIE, GCAE-AIE = Glaciated Clouds Albedo-Emissivity AIE.*

of the indirect effects of aerosols on glaciated clouds. The third cluster (the glaciated clouds lifetime (GCL-AIE)) provides the lifetime indirect effects for (green) glaciated (-4.08 $\pm$0.61 Wm^{-2}), (magenta) ice-only (-2.96 $\pm$0.44 Wm^{-2}) and (blue) mixed-phase (-1.42 $\pm$0.21 Wm^{-2}) clouds. These lifetime effects are derived by subtracting the corresponding albedo-emissivity effects of glaciated clouds (GCAE-AIE), which are given in the last cluster (derived from test A) from their corresponding counter-parts in the second cluster.

For our mesoscale area over Oklahoma, in which cloud cover is dominated by glaciated clouds aloft (Figs. 8 and Figs. 9), the aerosol indirect effect of glaciated clouds is stronger than that of water-only clouds. Globally, by contrast, the generally accepted hypothesis from previous studies states that, warm clouds make the largest contribution to the net radiative properties of all clouds, hence, to the indirect effects of aerosols as well (e.g. Charlson et al. (1992); Hobbs (1993); Gettelman et al. (2012)). This striking outcome is a consequence of the fact that glaciated clouds in this study were more extensive and more sensitive to aerosol changes in terms of horizontal coverage and domain-wide optical properties (7, Figs. 8 and 9) relative to liquid-only clouds.

Concerning the glaciated clouds indirect effects, surprisingly, it is noticeable that ice-only clouds exhibit a higher aerosol indirect effect than mixed-phase clouds, despite that the increase of the domain-averaged optical depth of ice-only clouds was less than that of mixed-phase clouds. The reason is that the sunlight is reflected first by ice-only clouds and dominance of short-wave effects over long-wave ones. The lifetime effect of ice-only clouds also dominates the glaciated clouds aerosol indirect effect.

4.1. *All Clouds*

4.1.1. *Negative net aerosol indirect effect from all clouds*

The net negative radiative flux change of -9.46 $\pm$1.4 Wm^{-2} at the TOA (Fig. 13) clearly shows that aerosol effects on clouds have the potential to offset the global warming exerted by greenhouse gases. Several factors augmented this outcome. The dominant pathway being; an increase in solute aerosols boosts the CCN loading and consequently, the number concentration of droplet embryos rises (Fig. 1a). Since the aerosol loading has minimal effect on the mean water content of a cloud, it is therefore apparent that the mean droplet size diminishes (Fig. 1b). Tiny but numerous cloud particles reflect more shortwave fluxes back to space, through the cloud-albedo indirect effect.

In addition, the precipitation efficiency of liquid-only clouds is reduced (Fig. 5), leading to a prolonged lifetime of the clouds and hence, the enhancement of chances of homogeneous freezing of cloud droplets, which boosts ice crystal concentrations aloft (Fig. 1c). These complementary factors lead to increased cloud coverage (Fig. 8 and 9) causing a reduction of solar radiation transmitted into the climate system. The vertical cloud fractions (plots not shown) underlined that this escalation of the cloud fraction is predominantly via stratiform type clouds, particularly mixed-phase clouds. Also, the optical thickness of the clouds in the present-day deepened (Fig. 7).

4.2. *Glaciated Clouds*

4.2.1. *Glaciated Clouds AIE Greater Than Water Clouds AIE*

The term glaciated clouds in this study refers to clouds comprised of ice crystals, either in their mixed- or ice-only cloud phases. The glaciated clouds aerosol indirect effect (GC-AIE = -6.33) is apparently stronger than the indirect effect from water-only clouds (WC-AIE = -3.13 $\pm$0.5 Wm^{-2}). From Figs. 1b, 1d, and 3, it is noticeable that water clouds exhibit a larger conditionally averaged optical thickness than glaciated clouds, because of higher water contents and relatively small droplet radii compared to glaciated clouds (Brient and Bony 2012); however, liquid-only clouds have a small horizontal coverage.

In this case study, liquid-only clouds contributed a small proportion to the whole cloud mass. Thus, their contribution to the total optical properties of clouds was small. This is expected for a tropical case where forced glaciation due to the prevalence of strong convective updrafts and generation of a glaciated layer-cloud by detrainment of ice is likely. Another factor is that glaciated clouds were more sensitive to aerosol changes than liquid-only clouds. Additionally, glaciated clouds exist above water-only clouds; hence, they have the first interaction with solar radiation before it reaches the water-only clouds below them.

The dominant mechanism giving rise to this result is the strong modification of glaciated clouds by homogeneous freezing of cloud droplets and solute aerosols and the subsequent detrainment of cloud ice from convective cores into stratiform/cirrus clouds.

4.2.2. *Ice-Only Clouds AIE Greater Than Mixed-Phase Clouds AIE*

In the second cluster of the bar charts, the presented aerosol indirect effects of glaciated clouds show a negative flux change (-6.33 $\pm$0.95 Wm^{-2}) due to aerosol pollution for both the lifetime and albedo-emissivity effects. Ice-only clouds have a higher flux change (-4.14 $\pm$0.61 Wm^{-2}) than mixed-phase clouds (-2.49 $\pm$0.41 Wm^{-2}). This finding brings into focus, novel insights into the higher importance of ice-only clouds in determining the net indirect effects of clouds. This higher importance of ice-only clouds is derived from their existence above mixed-phase clouds and hence, their first interaction with downward solar radiation. The ice-only cloud and mixed-phase clouds are produced by outflow from convective clouds, so they tend to overlap in the vertical. Also, the absolute increase of the volumetric cloud fraction of ice-only clouds is actually higher than that of mixed-phase clouds (Fig. 9) so that as well as being more extensive, ice-only clouds have also become deeper.

4.2.3. *Lifetime effect*

The lifetime aerosol indirect effects for glaciated clouds (GCL-AIE, -4.08 $\pm$0.57 Wm^{-2}) presented in the third cluster of the bar-charts show that the lifetime effect of mixed-phase clouds (-1.42 $\pm$0.18 Wm^{-2}) is about half that of ice-only clouds (-2.96 $\pm$0.41 Wm^{-2}). Despite the predicted greatest increase of cloud fractions for mixed-phase clouds (Fig. 8). The same arguments explained above, also explain this result.

4.2.4. *The Albedo Effect*

A negative flux change (solar cooling) for the albedo-emissivity effect due to aerosol pollution of glaciated clouds was predicted here (-2.25 $\pm$0.3 Wm^{-2}). This is mostly controlled by an increase in both droplet and ice crystal number concentrations followed by a reduction in mean sizes of cloud particles (Figs. 1d and 1b). Despite the fact that mean sizes of ice crystals are greater than those of water droplets by over a factor of four, ice-only clouds exhibit a slightly stronger albedo-emissivity effect (-1.18 $\pm$0.18 Wm^{-2}) compared to mixed-phase clouds (-1.07 $\pm$0.16 Wm^{-2}), primarily because of the massive increase in number concentrations of ice crystals and also the extent of ice-only clouds, which enhanced their reflectivity. Also, their first interaction with solar radiation makes them more important.

4.3. *Mixed-Phase Clouds*

The net flux change of the aerosol indirect effect of mixed-phase clouds is negative (-2.49 $\pm$0.41 Wm^{-2}), implying a cooling effect on the climate system. Now, in order to have a subtle understanding of the microphysical processes that control aerosol indirect effects in mixed-phase clouds, further sensitivity tests were carried out (Tests B and C).

4.3.1. *Coalescence Effect*

It was discovered that the liquid component of mixed-phase clouds exhibits a smaller indirect effect (-0.83 $\pm$0.12 Wm^{-2}) compared to the ice component (-1.66 $\pm$0.27 Wm^{-2}). This smaller contribution from the liquid relative to the ice component is attributed to the reduction in the effectiveness of the collision and coalescence of cloud droplets, and it yields a new indirect effect called coalescence indirect effect caused chiefly by the reduction of the mean sizes of cloud droplets, which inhibits coalescence and boosts the cloud lifetime (Fig. 1b). This is evidenced by the reduction in rain production in the mixed-phase clouds (Fig. 4a) and the conspicuous increase of the cloud fraction and optical thickness of mixed phase clouds due to aerosol pollution (Figs. 8, 9 and 10).

4.3.2. *Aggregation Effect*

The aggregation indirect effect is an aerosol indirect effect that arises from the response of the aggregation process of clouds to changes in aerosol loadings. It was assessed by the use of look-up

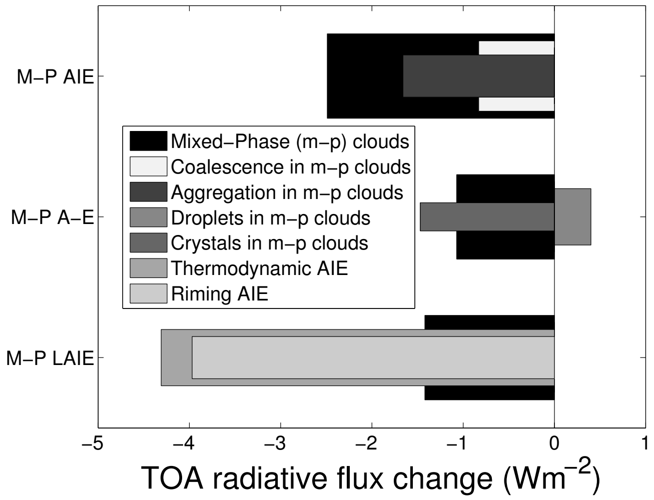

Figure 14. *Radiation statistics for mixed-phase clouds. The meanings of the abbreviations: M-P AIE = mixed-phase aerosol indirect effects (including both lifetime and albedo/emissivity effects), M-P A-E = Mixed-phase albedo emissivity effects, M-P LAIE = Mixed-phase lifetime aerosol indirect effects, ICAIE = Ice clouds aerosol indirect effects.*

table of the mean sizes of ice crystals in completely mixed-phase clouds. The dominant mechanism for the exhibited negative sign (-1.66 $\pm$0.25 Wm^{-2}) is the reduction of the mean sizes of ice crystals, which reduces the aggregation efficiency and increases the lifetime and extent of glaciated clouds.

4.3.3. *The Riming Aerosol Indirect Effect*

The TOA flux change of the riming indirect effect in Fig. 14 is strongly negative (-3.97 $\pm$0.61 Wm^{-2}), implying a cooling of the climate system. This arose from the inhibition of the growth of solid hydrometeors through poor accretion of supercooled cloud droplets by graupel or snow particles, thus prolonging the lifetime of mixed-phase clouds. In this study, a great reduction in cloud droplet sizes was caused by aerosol pollution and it led to significant reduction in graupel production and this emerged to be the dominant microphysics mechanism for the riming aerosol indirect effect.

4.3.4. *The Freezing-Related Thermodynamic Aerosol Indirect Effect*

Figure 14 shows a negative flux change at the TOA from the freezing-related thermodynamic aerosol indirect effect, which was inferred from Test D. More aerosols delayed the onset of precipitation and hence the cloud grew deeper until it reached freezing levels. The numerous cloud droplets consequently froze homogeneously prompting the release of vast amounts of latent heat that tend to invigorate the dynamics of clouds. There is however, weak evidence for this release of latent heat during freezing of cloud droplets. This is seen in the strengthening of both weak updraft and weak downdraft (Figs. 6c and 6d). This invigoration effect then intensifies the ice crystal processes as seen by the intensification of snow production aloft and may shorten the cloud lifetime.

Both the thermodynamic and riming indirect effects are individually much stronger than the net indirect effect of glaciated clouds. This is not the first time that such a response has been noted, the latest report of the IPCC (the fifth assessment report Boucher and Randall (2013)) compiled evidence from several modelling studies and concluded that individual indirect effects interact and compensate each other, hence the resultant aerosol indirect effect from clouds may not be reflective of what the individual effects show. Also, Lohmann and Feichter (2005) suggested that the individual aerosol indirect effects may not be necessarily additive.

4.3.5. *Albedo Effect*

Remarkably, the reflectivity of ice crystals within mixed-phase clouds dominated the albedo-emissivity effect therein, exhibiting a negative radiative flux change (-1.47 $\pm$0.22 Wm^{-2}) at the TOA, which was attributed to the massive increase in number concentrations of ice crystals and the reduction in mean sizes of ice crystals in mixed-phase clouds. Also, smaller particles interact with more radiation than the same water in bigger particles. On the other hand, the albedo-emissivity effect of water droplets within mixed-phase clouds surprisingly had a slight warming effect (0.4 $\pm$0.12 Wm^{-2}).

4.4. *Ice-Only Clouds*

Due to the higher importance of ice-only clouds (-4.14 $\pm$0.67 Wm^{-2}) compared to mixed-phase clouds (-2.49 $\pm$0.41 Wm^{-2}) in controlling the aerosol indirect effects in glaciated clouds, further sensitivity test were carried out to disentangle the individual contributions of each microphysical process involved. This was done by performing separate pairs of runs, with mean sizes of ice crystals in targeted microphysical processes of ice-only clouds being fixed. The identified processes were aggregation (-15.31 $\pm$2.29 Wm^{-2}), sedimentation (-1.37 $\pm$0.21 Wm^{-2}), and auto-conversion (-8.53 $\pm$1.28 Wm^{-2}). All these processes become less efficient in the present-day and hence, increasing the lifetime of ice-clouds.

Surprisingly, the results show that the sum of the indirect effects of each of these individual microphysical processes is not comparable to the net aerosol indirect effect of ice-only clouds – the individual indirect effects are much larger (Fig. 15). This discrepancy arises because of the limitation of sensitivity tests as a way of determining relative contributions from different processes to the overall flux change. Sensitivity tests cause perturbation of many processes, with compensating responses beyond the impact on the target process. Fig. 15 shows that the aggregation of ice particles became less prolific due to smaller ice crystals, reducing precipitation and increasing the cloud extent.

4.4.1. *Albedo/emissivity*

Due to the increase in ice crystal number concentrations in the present-day scenario and the consequent reduction in the effective sizes of ice crystals, the albedo-emissivity effect of ice-only

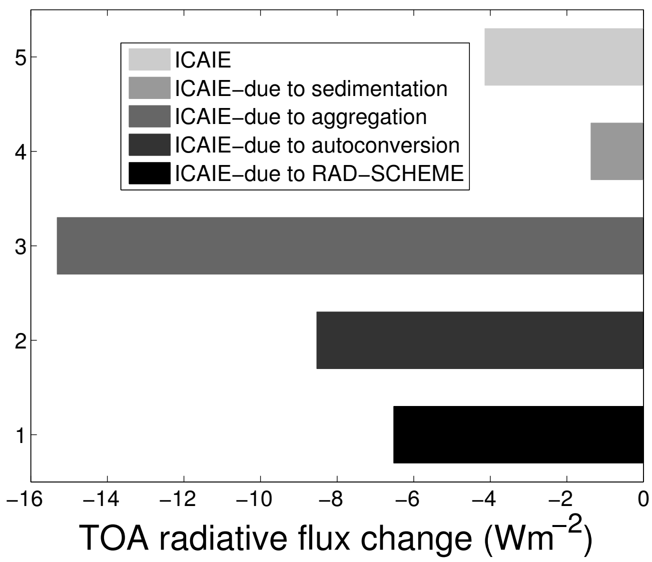

Figure 15. *Radiation statistics of ice-only clouds.*

clouds caused a negative radiative flux change at the TOA (-1.18 $\pm$0.18 Wm^{-2}), causing a cooling in the present-day climate (Fig. 13).

5. Conclusions

The sensitivity tests performed in this work improved the understanding of the responses of clouds micro-/macro- physical and dynamical properties to changes in aerosol chemistry and loading that has resulted mainly from anthropogenic activities. The simulations have showed that solute aerosol pollution has approximately doubled the cloud droplet number concentrations, although the factor by which the droplet concentration increased was about half of that for the pollution aerosol concentration. The extra cloud droplets then competed for the available vapour, and hence, the mean sizes of cloud droplets diminished by about 20%. Naturally, numerous cloud droplets do not promote precipitation production since they have poor aerodynamic interaction with each other. Also, crystal concentrations rose sharply above the -36°C level, owing to homogeneous freezing of cloud droplets and solute aerosols. Significant increase in LWC was also predicted, while IWC diminished in the upper troposphere due to solute aerosol pollution.

The hypothesis that solute aerosols modify glaciated clouds via homogeneous freezing was proved in this work when the ice crystal number concentrations aloft were amplified by the increases in the solute aerosol number concentrations. This increase in ice crystal number concentrations prevailed despite that solute aerosols are not allowed to nucleate ice heterogeneously in this aerosol-model. The ice number budget of the nucleation sources of ice crystals was conducted and homogeneous freezing of cloud droplets and aerosols, especially of sulphate aerosols was found to be the major sources of cloud ice, as found by Phillips et al. (2007). Other potential sources of ice crystals such as the Hallett-Mossop processes were surprisingly diminished in the present-day, owing to weaker riming than in the pre-industrial era. The effective mean sizes of ice crystals were subsequently reduced in the upper troposphere as a consequence of increased competition for available vapor. However, in mixed-phase clouds, an increase of the mean sizes of ice-crystals was noted.

A significant reduction in rain production was noted in the present-day and the dominant mechanism causing this reduction was the reduced efficiency of the collision-coalescence process owing to the reduction in the mean sizes of the cloud particles. Another cause for the reduction in rain production was discovered as the repartitioning of this precipitation type to the snow. This pathway was facilitated by the multiplication of ice-crystals owing to the proliferation of homogeneous freezing and growth by the 'Bergeron-Findeisen' process in the present day. The production of graupel in the present-day simulation was however found to have diminished mainly due to the reduction in the mean sizes of cloud droplets that rime onto ice and snow particles.

A general weakening of strong convection was noted in the present-day free troposphere owing to increased gravitational burden rendered by increased condensate loading. There was also a general reduction in atmospheric in upper-tropospheric relative humidity resulting mainly from the increased uptake of vapour by extra cloud particles.

On the macrophysical properties of the clouds, present-day clouds were more horizontally extensive, mainly mixed-phase clouds, primarily because riming and aggregation were less efficient in the polluted scenario. This weakening of precipitation producing processes causes the extension of the life span of a cloud giving rise to the lifetime effect of aerosols. Another striking discovery was the proliferation of glaciated clouds in the present-day, especially mixed phase clouds. Overall, the fraction and optical thickness of clouds were higher because of weak precipitation production in the polluted case. In summary, ice only clouds were found to be deeper than mixed-phase clouds in the present day than in the pre-industrial times.

It should be noted that the accuracy and consistency of these and related results are dependent on the nature of the models and the parameterizations used. Also, the nature of the large-scale forcing and the assumptions used in prescribing the aerosol profiles are important parameters in determining these results.

The predicted total aerosol indirect effect was equal to $-9.46 \pm 1.4 Wm^{-2}$, while the AIEs of glaciated clouds ($-6.33 \pm 0.95 Wm^{-2}$) were greater than those of water-only clouds

($-3.13 \pm 0.47Wm^{-2}$) by a factor of two in this continental case. The radiative importance of glaciated clouds lied in their large collective spatial extent that was higher than that water-only clouds. Also, their existence above water-only clouds renders them more radiatively important than water-only clouds. In addition to the traditional AIEs (glaciation, riming and thermodynamic), sedimentation, aggregation and coalescence were new AIEs identified, this finding is closely related to the recent work of Fan et al. (2013), who noted that microphysical processes are crucial in modifying the macrophysical properties of clouds. Importantly, it was discovered that these individual AIEs interact, compensate and buffer each other, hence, the relative importance of the contributions from responses of various processes vary during the climate change. Generally, the results show that the anthropogenic injection of aerosols into the atmosphere has the potential of offsetting the effects of CO_2-induced global warming. This is because the dominant effect of anthropogenic aerosol pollution on clouds is to cool the Earth, which corroborates the findings of Gettelman et al. (2012). It was also discovered that shortwave radiation dominated the aerosol indirect effect when compared compared to the longwave radiation by more than 90 %. Below, a summary of the most important pathways of aerosol indirect effects is presented. On average, the predicted AIEs had a standard deviation of around 15% associated with them.

The most important pathways identified in this study by which solute aerosols modify clouds and their indirect effects are summarized as follows.

- Solute aerosol pollution raised the number concentrations of cloud droplets (sulphate aerosols being the dominant source of cloud droplets), causing the diminishing of the mean sizes of cloud droplets and the inhibition of the warm rain processes and hence, promoting homogeneous freezing of cloud droplets.
- Subsequently, more ice crystals were detrained into the stratiform/cirrus and mixed-phase clouds from convective cores, hence the number concentrations of ice crystals aloft increased sharply, reducing their mean sizes. Consequently, the extent and optical thickness of clouds especially of glaciated clouds increased with anthropogenic aerosol pollution.
- Results showed that the negative net AIE from all clouds was dominantly a consequence of increases in spatial extent and optical thickness of clouds caused mainly by the reduction in mean sizes of cloud particles.
- Results also showed that homogeneous freezing of extra cloud droplets and aerosols and the subsequent detrainment of cloud ice into stratiform clouds are the dominant mechanisms of AIE of glaciated clouds. (These mechanisms are responsible for the higher sensitivity to aerosol changes of glaciated clouds compared to water-only clouds, because of this phenomenon, glaciated clouds emerged as more important in AIE of clouds compared to water-only clouds).

Acknowledgement

The work was funded by an award to, and directed by Vaughan T. J. Phillips (VTJP) from Office of Science (BER), US Department of Energy (DE-SC0002383, which later became DE-SC0007396). The authors are also grateful to the anonymous reviewers for their constructive criticism.

References

Albrecht, B., 1989: Aerosols, cloud microphysics, and fractional cloudiness, science. *Science*, **245 (4923)**, 1227–1230.

Andreae, M. O. and P. Merlet, 2001: Emission of trace gases and aerosols from biomass burning. *Global biogeochemical cycles*, **15 (4)**, 955–966.

Andreae, M. O. et al., 2007: Aerosols before pollution. *Science(Washington)*, **315 (5808)**, 50–51.

Baker, M. B. and T. Peter, 2008: Small-scale cloud processes and climate. *Nature*, **451 (7176)**, 299–300.

Bony, S. and J.-L. Dufresne, 2005: Marine boundary layer clouds at the heart of tropical cloud feedback uncertainties in climate models. *Geophysical Research Letters*, **32 (20)**.

Boucher, O. and D. Randall, 2013: Climate change 2013: The physical science basis. contribution of working group i to the fifth assessment report of the intergovernmental panel on climate change, (ipcc). *Cambridge University Press, Cambridge, United Kingdom and New York, NY, USA.*, **5th**.

Brient, F. and S. Bony, 2012: How may low-cloud radiative properties simulated in the current climate influence low-cloud feedbacks under global warming-. *Geophysical Research Letters*, **39**, L20 807.

Charlson, R., S. E. Schwartz, J. Hales, R. Cess, J. J. Coakley, H. JE., and H. DJ., 1992: Climate forcing by anthropogenic aerosols. *Science*, **255 (5043)**, 423–30.

Costantino, L. and F. M. Br9on, 2013: Aerosol indirect effect on warm clouds over south-east atlantic, from co-located modis and calipso observations. *Atmospheric Chemistry and Physics*, **13**, 69–88.

Cui, Z., K. S. Carslaw, Y. Yin, and S. Davies, 2006: A numerical study of aerosol effects on the dynamics and microphysics of a deep convective cloud in a continental environment. *J. Geophys. Res.*, **111 (D05)**, D05 201.

Cziczo, D. J., D. M. Murphy, P. K. Hudson, and D. S. Thomson, 2004: Single particle measurements of the chemical composition of cirrus ice residue during crystal-face. *J. Geophys. Res*, **109**, D04 201.

DeMott, P. J., et al., 2011: Resurgence in ice nuclei measurement research. *Bull. Amer. Meteor. Soc*, **92**, 1623–1635.

Diehl, K., S. Matthias-Maser, R. Jaenicke, and S. Mitra, 2002: The ice nucleating ability of pollen:: Part ii. laboratory studies in immersion and contact freezing modes. *Atmospheric research*, **61 (2)**, 125–133.

Diehl, K., C. Quick, S. Matthias-Maser, S. Mitra, and R. Jaenicke, 2001: The ice nucleating ability of pollen: Part i: Laboratory studies in deposition and condensation freezing modes. *Atmospheric Research*, **58 (2)**, 75–87.

Dymarska, M., B. J. Murray, L. Sun, M. L. Eastwood, D. A. Knopf, and A. K. Bertram, 2006: Deposition ice nucleation on soot at temperatures relevant for the lower troposphere. *Journal of Geophysical Research: Atmospheres (1984–2012)*, **111 (D4)**.

Eidhammer, T., P. J. DeMott, and S. M. Kreidenweis, 2009: A comparison of heterogeneous ice nucleation parameterizations using a parcel model framework. *Journal of Geophysical Research: Atmospheres (1984–2012)*, **114 (D6)**.

Fan, J., L. R. Leung, D. Rosenfeld, Q. Chen, Z. Li, J. Zhang, and H. Yan, 2013: Microphysical effects determine macrophysical response for aerosol impacts on deep convective clouds. *Proceedings of the National Academy of Sciences*, **110 (48)**, E4581–E4590.

Fan, J., D. Rosenfeld., L. Yanni Ding, R. Leung., and Z. Li, 2012: Potential aerosol indirect effects on atmospheric circulation and radiative forcing through deep convection. *Geophysical Research Letters*, **39 (9)**, L09 806.

Freidenreich, S. M. and V. Ramaswamy, 1999: A new multiple-band solar radiative parameterization for general circulation models. *J. Geophys. Res*, **104 (D24)**, 31 389–31 409.

Gao, R., et al., 2004: Evidence that nitric acid increases relative humidity in low-temperature cirrus clouds. *Science*, **303 (5657)**, 516–520.

Gettelman, A., X. Liu, D. Barahona, D. Lohmann, and C. Chen, 2012: Climate impacts of ice nucleation. *Journal of Geophysical Research: Atmospheres*, **117 (D20)**, D20 201.

Haywood, J. and O. Boucher, 2000: Estimates of the direct and indirect radiative forcing due to tropospheric aerosols: A review. *Reviews of Geophysics*, **38 (4)**, 513–543.

Haywood, J., L. Donner, A. Jones, and J.-C. Golaz, 2009: *Global indirect radiative forcing caused by aerosols: IPCC (2007) and beyond In Clouds in the Perturbed Climate System*. MIT Press (In Clouds in the Perturbed Climate System), 451-467 pp.

Hill, A. A. and S. Dobbie, 2008: The impact of aerosols on non-precipitating marine stratocumulus. ii: The semi-direct effect. *Quarterly Journal of the Royal Meteorological Society*, **134**, 1155–1165, doi:10.1002/qj.277.

Hobbs, P. V., 1993: *Aerosol-cloud-climate interactions*, Vol. 54. Academic Press.

Hoeve, T. J. E., L. A. Remer, and M. Z. Jacobson, 2011: Microphysical and radiative effects of aerosols on warm clouds during the amazon biomass burning season as observed by modis: impacts of water vapor and land cover. *Atmos. Chem. Phys.*, **11**, 3021–3036.

Hoppel, W. A., G. M. Frick, and J. W. Fitzgerald, 2002: Surface source function for sea-salt aerosol and aerosol dry deposition to the ocean surface. *Journal of Geophysical Research: Atmospheres*, **107 (D19)**, AAC 7–1–AAC 7–17, doi:10.1029/2001JD002014, URL http://dx.doi.org/10.1029/2001JD002014.

Johnson, B., K. Shine, and P. Forster, 2004: The semi-direct aerosol effect: Impact of absorbing aerosols on marine stratocumulus. *Quarterly Journal of the Royal Meteorological Society*, **130 (599)**, 1407–1422.

Johnson, B. T., 2003: The semi-direct aerosol effect. Ph.D. thesis, The University of Reading.

Koch, D. and A. D. Genio, 2010: Black carbon semi-direct effects on cloud cover: review and synthesis. *Atmospheric Chemistry and Physics*, **10 (16)**, 7685–7696.

Korolev, A., 2007: Limitations of the wegener-bergeron-findeisen mechanism in the evolution of mixed-phase clouds. *J. Atmos. Sci*, **64**, 3372–3375, doi: http://dx.doi.org/10.1175/JAS4035.1.

Kudzotsa, I., 2013: Mechanisms of aerosol indirect effects on glaciated clouds simulated numerically. Ph.D. thesis, University of Leeds, UK.

Kudzotsa, I., et al., 2016: Aerosol indirect effects on glaciated clouds. part i: Model description. *QJRMS*.

Lamb, D. and J. Verlinde, 2011: *Physics and Chemistry of Clouds*. Cambridge University Press.

Leaitch, W. R., G. A. Isaac, J. W. Strapp, C. M. Banic, and H. A. Wiebe, 1992: The relationship between cloud droplet number concentrations and anthropogenic pollution: Observations and climatic implications. *J. Geophys. Res.*, **97 ((D2)**, 2463–2474.

Liao, H. and J. H. Seinfeld, 1998: Effect of clouds on direct aerosol radiative forcing of climate. *Journal of Geophysical Research: Atmospheres (1984–2012)*, **103 (D4)**, 3781–3788.

Liou, K. N., 2002: *An introduction to atmospheric radiation*. Academic Press.

Lohmann, U. and J. Feichter, 2001: Can the direct and semi-direct aerosol effect compete with the indirect effect on a global scale? *Geophysical Research Letters*, **28 (1)**, 159–161.

Lohmann, U. and J. Feichter, 2005: Global indirect aerosol effects: a review. *Atmospheric Chemistry and Physics*, **5 (3)**, 715–737, doi:10.5194/acp-5-715-2005, URL http://www.atmos-chem-phys.net/5/715/2005/.

Lohmann, U., et al., 2010: Total aerosol effect: radiative forcing or radiative flux perturbation-. *Atmospheric Chemistry and Physics*, **10 (7)**, 3235–3246, doi:10.5194/acp-10-3235-2010, URL http://www.atmos-chem-phys.net/10/3235/2010/.

Martin, G., D. Johnson, and A. Spice, 1994: The measurement and parameterization of effective radius of droplets in warm stratocumulus clouds. *Journal of the Atmospheric Sciences*, **51 (13)**, 1823–1842.

Meyers, M. P., P. J. DeMott, and W. R. Cotton, 1992: New primary ice-nucleation parameterizations in an explicit cloud model. *Journal of Applied Meteorology*, **31 (7)**, 708–721.

Miller, M. A., 2007: Sgp cloud and land surface interaction campaign (clasic): Science and implementation plan. *DOE/SC-ARM-0703*.

Morrison, H. and W. W. Grabowski, 2011: Cloud-system resolving model simulations of aerosol indirect effects on tropical deep convection and its thermodynamic environment. *atmospheric chemistry and physics*, **11**, 10 503–10 523, doi:10.5194/1cp-11-10503-2011.

O'Donnell, D., K. Tsigaridis, and J. Feichter, 2011: Estimating the direct and indirect effects of secondary organic aerosols using echam5-ham. *Atmos. Chem. Phys.*, **11**, 8635–8659.

Pandithurai, G., et al., 2009: Aerosol effect on cloud droplet size as monitored from surface-based remote sensing over east china sea region. *Geophys. Res. Lett*, **36**, L13 805, doi:10.1029/2009GL038451.

Phillips, V. T. J., C. Andronache, B. C. E. Morris, D. C. Sands, A. Bansemer, A. Lauer, C. McNaughton, and C. Seman, 2009: Potential impacts from biological aerosols on ensembles of continental clouds simulated numerically. *Biogeosciences*, **6**, 987–1014.

Phillips, V. T. J., T. W. Choularton, R. J. llingworth, A. J. Hogan, and P. R. Field, 2003: Simulations of the glaciation of a frontal mixed-phase cloud with the explicit microphysics model. *Quarterly Journal of the Royal Meteorological Society*, **129 (590)**, 1351–1371, doi:10.1256/qj.02.100.

Phillips, V. T. J., P. J. DeMott, and C. Andronache, 2008: An empirical parameterization of heterogeneous ice nucleation for multiple chemical species of aerosol. *Journal of the atmospheric sciences*, **65**, 2757–2783, doi:10.1175/2007JAS2546.1.

Phillips, V. T. J., P. J. Demott, C. Andronache, K. A. Pratti, and C. Twohy, 2013: Improvements to an empirical parameterization of heterogeneous ice nucleation and its comparison with observations. *J. Atmos. Sci.*, **70**, 378–409.

Phillips, V. T. J., L. J. Donner, and S. T. Garner, 2007: Nucleation processes in deep convection simulated by a cloud-system-resolving model with double-moment bulk microphysics. *Journal of the Atmospheric Sciences*, **64**, 738–761, doi:http://dx.doi.org/10.1175/JAS3869.1.

Ramanathan, V., et al., 2007: Atmospheric brown clouds: Hemispherical and regional variations in long-range transport, absorption, and radiative forcing. *Journal of Geophysical Research: Atmospheres (1984–2012)*, **112 (D22)**.

Salma, I. and W. Maenhaut, 2006: Changes in elemental composition and mass of atmospheric aerosol pollution between 1996 and 2002 in a central european city. *Environmental Pollution*, **143 (3)**, 479–488.

Solomon, S., D. Qin, M. Manning, Z. Chen, M. Marquis, K. Averyt, M.Tignor, and H. M. (eds.), 2007: Climate change 2007: The physical science basis. contribution of working group i to the fourth assessment report of the intergovernmental panel on climate change, (ipcc). *Cambridge University Press, Cambridge, United Kingdom and New York, NY, USA.*, **4th**.

Storer, R. L. and S. C. van den Heever, 2013: Microphysical processes evident in aerosol forcing of tropical deep convective clouds. *J. Atmos. Sci*, **70 (2)**, 430–446.

Streets, D. G., et al., 2003: An inventory of gaseous and primary aerosol emissions in asia in the year 2000,. *J. Geophys. Res*, **108 (8809)**, D21, doi:10.1029/2002JD003093.

Sun, Y., et al., 2004: The air-borne particulate pollution in beijing-concentration, composition, distribution and sources. *Atmospheric Environment*, **38 (35)**, 5991–6004.

Takemura, T., 2012: Distributions and climate effects of atmospheric aerosols from the preindustrial era to 2100 along representative concentration pathways (rcps) simulated using the global aerosol model sprintars. *Atmos. Chem. Phys.*, **12**, 11 555–11 572.

Twomey, S., 1974: Pollution and the planetary albedo. *Atmospheric Environment*, **8**, 1251–1256.

Twomey, S. A., 1977: The influence of pollution on the shortwave albedo of clouds. *Journal of the Atmospheric Sciences*, **34 (7)**, 1149–1152.

Watson, R., H. Rodhe, H. Oeschger, and U. Siegenthaler, 1990: Greenhouse gases and aerosols. *Climate change: the IPCC scientific assessment*, **1**, 17.

Zeng, X., et al., 2009: An indirect effect of ice nuclei on atmospheric radiation. *J. Atmos. Sci*, **66**, 41–61, doi:http://dx.doi.org/10.1175/2008JAS2778.1.

